Chemical Physics 353 (2008) 185–188

Contents lists available at ScienceDirect

Chemical Physics

journal homepage: www.elsevier.com/locate/chemphys

Terahertz study of trichloroanisole by time-domain spectroscopy

Yew Li Hor [a], Hee C. Lim [a], John F. Federici [a,*], Eric Moore [b], Joseph W. Bozzelli [b]

[a] Department of Physics, New Jersey Institute of Technology, Newark, NJ 07102, USA
[b] Department of Chemistry, New Jersey Institute of Technology, Newark, NJ 07102, USA

ARTICLE INFO

Article history:
Received 14 February 2008
Accepted 20 August 2008
Available online 23 August 2008

Keywords:
Trichloroanisole
2,4,6-Trichloroanisole
2,3,4-Trichloroanisole
2,5,6-Trichloroanisole
Terahertz
Cork taint
Spectroscopy
Internal rotor

ABSTRACT

The THz transmission spectra of three trichloroanisole (TCA) compounds (2,3,4-TCA, 2,4,6-TCA and 2,5,6-TCA) are measured using terahertz time-domain spectroscopy (THz-TDS). The spectrum of 2,4,6-TCA in the solid phase displays several discrete absorption peaks over frequency range from 0.1 to 1.5 THz, with significant peaks observed at 0.6, 0.95 and 1.2 THz. A weak absorption peak is observed near 0.2–0.3 THz. Computational chemistry using the B3LYP density functional method is used to study structure and internal rotations in 2,4,6-TCA, where results strongly suggest that frequencies of the CH_3O–carbon(benzene) internal rotor of the methoxy group correspond to the observed spectra.

1. Introduction

Isomers of trichloroanisole (TCA, trichloro-methoxy benzene), with molecular formula $C_7H_5OCl_3$, are reported to be present as contaminants in a number of foods and beverages. Is it reported to effect the muddy favor in drinking water [1,2], and be present in sake, rice [3] and raisins [4]. 2,4,6-TCA is also thought to be the main compound responsible for cork taint in wine [5,6]. TCA has also been recognized as the source for musty odors in indoor pollution studies [7]. A small amount of 2,4,6-TCA could badly contaminate foods and beverages. For example, the consumer rejection threshold (CRT) of wine is 3.1 ppt [8]. As an indoor pollutant, 2,4,6-trichloroanisole is perceptible at extremely low concentrations in a range of 5–10 ppt in air [7].

The formation of 2,4,6-TCA involves a series of complex chemical reaction paths. One well-reported overall mechanism is the conversion of 2,4,6-chlorophenols to 2,4,6-chloroanisole by microscopic fungi such as *Aspergillus, Fusarium* and *Penicillium*, which are found in wood and other humid or high-moisture environments [9]. Since chlorophenols have been used as pesticides and wood preservatives, the uptake of the minutest amounts of chlorophenol by cork tree bark during its growth, or during subsequent manufacture into cork provides a production potential for TCA. The cork bleaching agent, hypochlorite, also provides a chemical source for eventual formation of chlorophenols. The presence of TCAs in tap water is reported to result from trichlorophenols formed during chlorine disinfection of drinking water, where subsequent methylation occurs in the distribution system [10]. TCAs may also be formed in packing materials and wooden shipping container floors [2].

The interaction of terahertz (THz) radiation with materials depends in part on the material's phase: solid, liquid or gas [11]. For gas-phase molecules, rotational and vibrational states typically occupy the THz region. Molecules which are polar, such as water vapor, exhibit many spectral lines due to their strong interaction with the THz electric field. Non-polar molecules interact very little and are therefore transparent. For liquids, the rotational and vibrational excitations are strongly damped by the proximity of neighboring molecules. They are highly absorbing over a broad range of THz frequencies, thus generally yielding broad and continuum THz spectra. The THz absorption spectra of crystalline solids can result from both intra-molecular vibrations as well as from large-scale intermolecular vibrational motion of the crystal structure.

As emphasized in recent papers on modeling of THz spectra of solid-state [12], calculations on isolated molecules generally do not accurately predict vibrational modes in the THz region. In such systems, the periodic crystal structure is critical even for predicting the lowest energy vibration modes. Ref. [12] describes an ab initio simulation method which utilizes a plane-wave pseudopotential approach within the density functional formalism. This method incorporates the periodic crystal structure and can be used to identify the normal vibration modes in the THz region. While modeling of whole crystal structure rather then single molecule generally

* Corresponding author. Tel.: +1 973 596 8482.
E-mail address: federici@adm.njit.edu (J.F. Federici).

0301-0104/$ - see front matter © 2008 Elsevier B.V. All rights reserved.
doi:10.1016/j.chemphys.2008.08.011

may be required to provide further understanding of absorption modes in the terahertz spectra, in the case of TCA, the THz spectra appear not to be dominated by large-scale vibrational modes of the crystal, but rather by internal methoxy rotors. In this paper, we investigate the THz spectrum of TCA using both THz-TDS as well as computationally using the B3LYP density functional method.

2. Experimental setup

TCA crystals were purchased from Sigma–Aldrich, Inc with 99% purity. The samples are prepared by grinding the TCA crystal into powder. The TCA powder is mixed with polyethylene at different mass ratios. Polyethylene is chosen for the mixture since it is fairly transparent in the THz range. Both the TCA and polyethylene grains are less then 100 μm as determined by sieving with a 100 μm mesh filter. The mixture is then pressed into a thin circular tablet 10 mm in diameter. Several samples with compositions by weight ranging from 0% (pure polyethylene) to 80% TCA were prepared.

A T-Ray 2000 Spectroscopy system (Picometrix, Inc) is used to measure the time-domain THz transmission of the sample. Further details of the THz time-domain method may be found in Ref. [13]. For the measurement, the THz radiation is focused to a ~3 mm spot size using silicon lenses. The room temperature TCA sample is placed at the focus. The THz radiation transmitted through the sample is averaged 30 times corresponding to a signal-to-noise ratio of ~50:1. The time-domain data are then Fourier transformed to yield a frequency power spectrum. Fig. 1 shows the E-field of the measured sample, polyethylene pellets and air both in time and frequency domain. The useful experiment bandwidth is 0.1–3.0 THz with no sample (air) while with polyethylene pellets, the usable bandwidth is slightly reduced to ~2.0 THz.

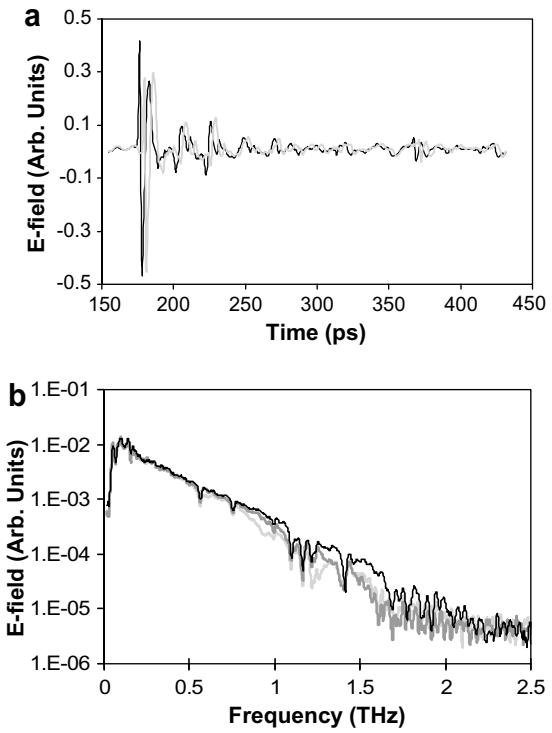

Fig. 1. (a) Measured THz time-domain waveform (light gray) through a 2.5 mm tablet of 50% 2,4,6-TCA/polyethylene. The reference waveform (black) is taken with the sample removed. (b) Corresponding amplitudes as a function of frequency after Fourier transforming the time-domain data. The dark gray curve is the measured transmission amplitude of a 2 mm thick pure polyethylene tablet.

3. Results and discussion

Both the absorption and real refractive index may be calculated from the time-domain measurements since the sample path length, d, is known. The complex transmission coefficient through a uniform material of complex index of refraction $\tilde{n}(\nu)$ can be calculated to be

$$t(\nu) = \frac{E_s(\nu)}{E_r(\nu)} = \frac{4\tilde{n}}{(\tilde{n}+1)^2}\frac{e^{i2\pi(\tilde{n}-1)\nu d/c}}{1+\beta} \tag{1}$$

where

$$\beta = \frac{(1-\tilde{n})^2}{(1+\tilde{n})^2}e^{i4\pi i\tilde{n}\nu d/c} \tag{2}$$

and $|E_s|$ and $|E_r|$ are the magnitudes of the THz electric fields for the sample and reference, respectively. Due to the strong absorbance of the sample, reflections within the sample are negligible to first approximation. In this limit, the term β in the denominator of Eq. (1) can be neglected. The complex refractive index can be express as

$$\tilde{n}(\nu) = n(\nu) + i\frac{\alpha(\nu)c}{2\pi\nu}. \tag{3}$$

where $n(\nu)$ is the real refractive index, $\alpha(\nu)$ defines the electric field absorption coefficient, c is the speed of light in vacuum, and ν is the frequency. By measuring both the phase and amplitude of the transmitted THz wave, Eqs. (1) and (3) can be used to extract the frequency-dependent real index of refraction and absorption coefficient.

Fig. 2 shows the effective absorption of the 2,4,6-TCA/polyethylene samples. Note that as the percent weight of the TCA relative to the polyethylene is decreased, the absorption peaks also decrease as expected. The strengths of spectral features near 1.5 THz are nebulous due to the limited dynamic range above 1.5 THz. As the THz frequency approaches 1.5 THz, the noise approaches the noise floor of the THz system.

Since the measured samples are a mixture of polyethylene and TCA, one must extract the absorption coefficient and index of refraction of TCA given the measured absorption coefficient and refractive index of the mixture and pure polyethylene. Based on a simple model which attributes the "effective" absorption coefficient and index of refraction to a weighted average of the composite materials, we can extract the attenuation coefficient of the TCA for each sample

$$\alpha_{eff} = V_{TCA}\alpha_{TCA} + V_{PE}\alpha_{PE} \tag{4}$$

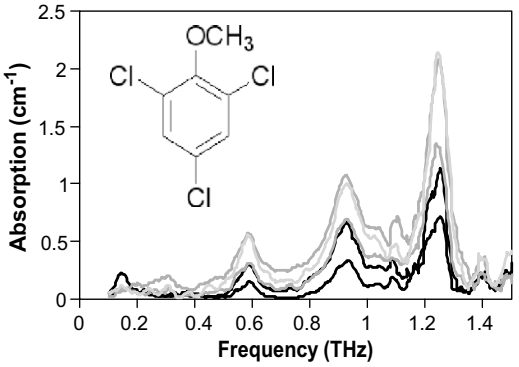

Fig. 2. Measured absorption of 2,4,6-TCA tablets. The relative concentration of TCA to PE varies from 40% TCA/60% PE (black) to 80% TCA/20% PE (light gray). Sharp features at 0.6, 0.95 and 1.25 THz are prominent. A weak but spectrally broad feature exists near 0.2–0.3 THz. Structure near 1.1 THz is an artifact of absorption by water vapor in the atmosphere.

where α_{eff} is the measured absorption coefficient of the composite material, V is the percentage volume of an individual component in the composite, α is the component absorption coefficient, and the subscript PE refers to polyethylene. We estimate the mass density of pure TCA and pure PE by individually compressing 330 mg of each compound. The mass density of the pressed 100% TCA tablet is 4.2 mg/mm^3 while the 100% pure PE tablet is 1.33 mg/mm^3. The percent volume of a TCA/PE mixture is calculated based on the mass density and weight of each component material assuming that the volume of air in the composite sample is negligible. For example, the 70% TCA/30% PE sample is comprised of 231 mg of TCA mixed with 99 mg of PE. The volume of 2,4,6-TCA in the sample is then 55.0 mm^3. A similar calculation gives the volume of polyethylene as 74.4 mm^3. The volume fractions for this tablet are $V_{TCA} = 42.5\%$ and $V_{PE} = 57.5\%$. As a check we note that the predicted combined volume (129.4 mm^3) is close to the volume of the sample (119 mm^3) as measured using a micrometer.

In order to extract the peak absorption coefficient for TCA, it is assumed that reflective losses from the air-sample interfaces are negligible compared to absorption loses near the 0.6, 0.95 and 1.25 THz absorption peaks. In this limit, the absorbance is related to the absorption coefficient by $\ln(1/T) = A = \alpha_{eff}L$ where L is the total thickness of the sample. For example, for the 70% TCA/30% PE sample, $\alpha_{eff} = 0.425 \times \alpha_{TCA} + 0.575 \times \alpha_{PE}$, where α_{PE} can be extracted from absorbance data from the pure polyethylene sample.

Based on the data for the various samples, the frequency-dependent absorption coefficient for the three isomers of TCA is shown in Fig. 3. Prominent absorption features at 0.6, 0.95 and 1.25 THz are observed. A weak and spectrally broad absorption feature near 0.2–0.3 THz is also observed as the percentage of TCA in the tablet is increased. By taking the average of the absorption coefficient values obtained for different TCA/polyethylene compositions, the absorption coefficient for 2,4,6-TCA is (0.98 ± 0.20) cm^{-1} at 0.6 THz, (1.97 ± 0.44) cm^{-1} at 0.95 THz and (3.87 ± 0.52) cm^{-1} at 1.25 THz. The spectrally broad feature near 0.2 THz has an absorption coefficient of approximately 0.2 cm^{-1}. In comparing the THz spectra of 2,4,6-TCA with the two isomers 2,3,4-TCA and 2,3,6-TCA, the THz spectra clearly depend on the chlorine location in the molecular structure.

In order to assign the observed absorption peaks to specific vibrational or rotational motion of the 2,4,6-trichloroanisole, the THz absorbance spectra are theoretically computed using density functional and ab initio computational methods. The geometries of reactants and structures through the internal rotation of the methoxy group are calculated at the B3LYP[8] functional with the Dunning polarized double zeta basis set using the Gaussian 03 program [14]. The internal rotation potential is calculated as a function of the C(H_3)–O–C_b–C_b dihedral. Energy levels are calculated by use of free rotor wave functions and solution of the S'Eqn by direct diagonalization of the Hamiltonian matrix of hindered internal rotation potential represented by the truncated Fourier series as $a_0 + \sum a_i \cos(i\varphi) + \sum b_i \sin(i\varphi)$ with $\varphi \leqslant 8$ [15,16].

If internal rotor analysis is not included in the calculation, the predicted THz absorption spectra (Fig. 4b, inset) do not resemble the measured THz spectra. However, when the CH_3O–C_b methoxy internal rotor is included, with a limited level population relative to that of a gas phase Boltzman population, the predicted THz spectra (Fig. 4a) roughly reproduce the equal frequency spacing of the observed 2,4,6-TCA THz absorption peaks. The peaks at 0.6, 0.95 and 1.25 THz can be clearly identified with similar peaks in the simulated spectra. The predicted peak at 0.25 THz may correspond to the experimentally observed broad spectral feature from ~0.2 to 0.3 THz. The predicted THz spectra are shifted to lower THz frequencies relative to the experimental spectra. The solid curve of Fig. 4b, which shows that the internal rotor analysis with the near full 2000 energy levels representative of a Boltzman distribution at room temperature for a gas phase molecule, does not well represent the experimental data. However, when we reduce the number of levels in the spectral analysis to only 1000 energy levels (dashed curves of Fig. 4a and b), the predicted spectra show a surprising good fit in comparison to the experimental data. It is interpreted that the barrier to rotation must be more hindered in the condensed phase and thus fewer energy levels populated in the condensed phase relative to the gas phase.

In comparing the THz spectra of the different isomers of TCA, it is observed that positioning of the chlorines on the benzene ring

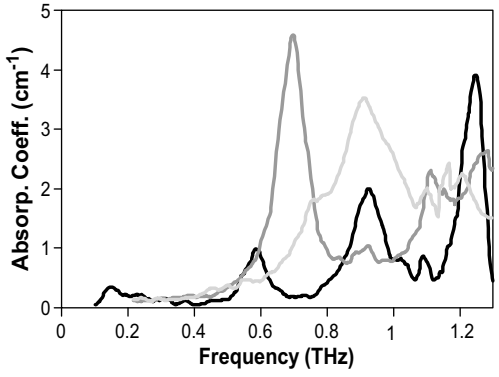

Fig. 3. Plot of the average extracted absorption coefficients for 2,4,6-TCA (black curve), 2,3,4-TCA (dashed dark gray) and 2,3,6-TCA (light gray).

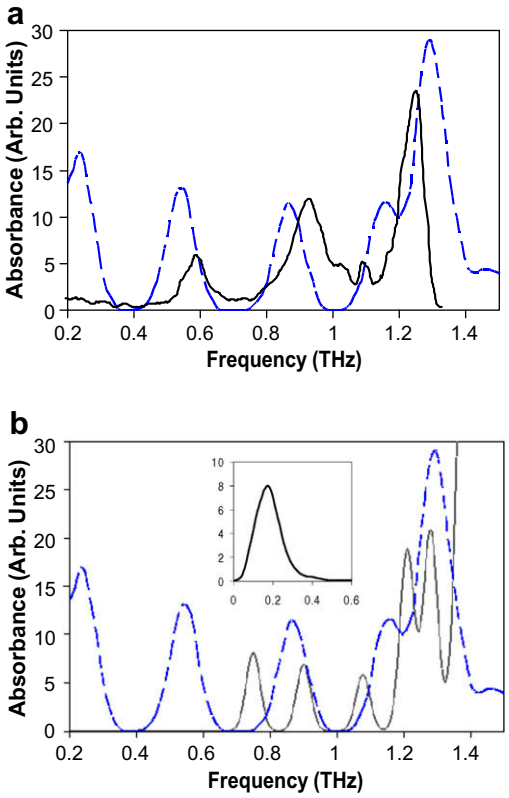

Fig. 4. (a) Predicted THz absorption spectra (dashed curve) for an isolated molecule of 2,4,6-TCA (dashed curve) using 1000 energy levels compared to experimentally measured 2,4,6-TCA spectra (solid curve) from Fig. 3. (b) Predicted THz absorption spectra (dashed curve) for an isolated molecule of 2,4,6-TCA (dashed curve) using 1000 energy levels compared to theoretical prediction with 2000 energy levels. Inset – predicted THz absorption spectra for 2,4,6-TCA in the absence of an internal rotor.

structure significantly changes the THz spectra. This effect is to be expected with the methoxy rotor since the location of the chlorines (e.g. 2,4,6 compared to 2,3,4) changes the barrier potential, and concomitantly the frequencies of the rotor. Moving the chlorine from the 6 position eliminates the twofold symmetry of the rotor. If the CH_3 rotor were responsible for the THZ spectra, one would not expect a dramatic change in the THz spectra with different isomers since the barrier potential of the CH_3 rotor would be much less sensitive to positioning of the chlorine. The results from the calculation on the 2,4,6 isomer combined with the structure suggest that the absorption peaks in the THz spectra of 2,4,6-TCA are due to the methoxy internal rotor.

While there is reasonably good agreement between theory and experiment, we cannot definitively rule out the possibility that the crystallinity or intermolecular vibrations may account for any discrepancies between the two. For example, 3,4-methylene-dioxymethamphetamine hydrochloride (Ecstasy) seems to be accurately modeled by single-molecule calculations. However, solid-state density functional theory simulations reveal [17] that while half of the experimentally observed THz absorption arises from single-molecule states, the other half arises from intra-molecular lattice vibrations. The relative frequency shift of the predicted 2,4,6-TCA spectra relative to the experimentally measured spectra could be due the effect of the TCA crystal structure relative to the gas phase calculated data. While the ab initio calculations assume that the molecules are isolated (gas phase), the THz measurements were conducted on solid phase samples. It has been suggested that the blue shifted frequencies of the experimental spectra compared to calculated spectra may result from a packing force and steric effect in the crystalline phase [18,19]. Conceptually, since the molecule is in a more rigid setting in the solid compared to gas phase, one would expect the vibrational modes of the rotor to stiffen corresponding to an upward shift in frequency relative to the gas phase modes.

An alternative explanation for the frequency shift could be due to an error in the calculated barrier potential of the rotor. At the low frequencies of interest, it is not unusual for the calculated barriers to be uncertain within 10–20%. This level of error could potentially shift the predicted energy levels and consequently the predicted THz absorbance spectra in frequency.

4. Conclusion

The THz spectral transmission of TCA compounds in 0.1–1.5 THz range has been measured and analyzed. The spectral dependence of the absorption for individual TCA isomers is extracted from the transmission data. 2,4,6-TCA exhibits three strong absorption peaks coefficient at 0.6, 0.95 and 1.25 THz. A weaker peak at 0.2–0.3 THz is observed for high volume fractions of TCA. THz measurements of the two other TCA isomers demonstrate that the chlorine placement has a significant impact on the THz spectra. While intermolecular interactions of the solid state may somewhat alter the predicted THz spectra, comparison of single molecule ab initio modeling with the measured THz spectra strongly suggests that the observed absorption peaks of 2,4,6-TCA are likely the result of a methoxy internal rotor.

Acknowledgements

Helpful discussions with K. Tandon and Profs. R. Barat and J. M. Joseph are gratefully acknowledged.

References

[1] A. Nystrom, A. Grimvall, C. Krantz-Rulcker, R. Savenhed, K. Akerstrand, Water Sci. Technol. 25 (1992) 241.
[2] S. Karlsson, S. Kaugare, A. Grimvall, H. Boren, R. Savenhed, Water Sci. Technol. 31 (1995) 99.
[3] A. Miki, A. Isogai, H. Utsunomiya, H. Iwata, J. Biosci. Bioeng. 100 (2005) 178.
[4] L.H. Aung, J.L. Smilanick, P.V. Vail, P.L. Hartsell, E. Gomez, J. Agric. Food Chem. 44 (1996) 3294.
[5] C. Silva Pereira, J.J. Figueiredo Marques, M.V. San Romao, Crit. Rev. Microbiol. 26 (2000) 47.
[6] A.P. Pollnitz, K.H. Pardon, D. Liacopoulos, G.K. Skouroumounis, M.A. Sefton, Aust. J. Grape Wine Res. 2 (1996) 184.
[7] J. Gunschera, F. Fuhrmann, T. Salthammer, A. Schulze, E. Uhde, Environ. Sci. Pollut. Res. 11 (2004) 147.
[8] J. Prescott, L. Norris, M. Kunst, S. Kim, Food Qual. Prefer. 16 (2005) 345.
[9] M.L. Álvarez-Rodríguez, L. López-Ocaña, J.M. López-Coronado, E. Rodríguez, M.J. Martínez, G. Larriba, J.-J.R. Coque, Appl. Environ. Microbiol. 68 (2002) 5860.
[10] T.H. Lee, R.F. Simpson, in: G.H. Fleet (Ed.), Wine Microbiology and Bio/Technology, G. Harwood Academic Publishers, Chur, Switzerland, 1993, p. 353.
[11] F.C. Delucia, in: D. Mittleman (Ed.), Sensing with Terahertz Radiation, Springer (2003).
[12] P. Uhd Jepsen, S.J. Clark, Chem. Phys. Lett. 442 (2007) 275.
[13] D. Mittleman, in: D. Mittleman (Ed.), Sensing with Terahertz Radiation, Springer (2003).
[14] M.J. Frisch, G.W. Trucks, H.B. Schlegel, G.E. Scuseria, M.A. Robb, et al., Gaussian 03, B.04 ed., Gaussian, Inc., Pittsburgh, PA, 2003.
[15] T.H. Lay, L.N. Krasnoperov, C.A. Venanzi, J.W. Bozzelli, N.V. Shokhirev, J. Phys. Chem. 100 (1996) 8240.
[16] N.V. Shokhirev, Quantum Rotator, <http://www.chem.arizona.edu/faculty/walk/nikolai/programs.html#rotor>, 1999.
[17] D.G. Allis, P.M. Hakey, T.M. Korter, International Symposium on Spectral Sensing Research, 2008, p. 147.
[18] G. Wang, J. Shen, Y. Ji, J. Appl. Phys. 102 (2007) 013106.
[19] Y. Chen, H. Liu, Y. Deng, D. Schauki, M.J. Fitch, R. Osiander, C. Dodson, J.B. Spicer, M. Shur, X.-C. Zhang, Chem. Phys. Lett. 400 (2004) 357.